Quantum effects in the capture of charged particles by dipolar polarizable symmetric top molecules. I. General axially nonadiabatic channel treatment

M. Auzinsh, E. I. Dashevskaya, I. Litvin, E. E. Nikitin, and J. Troe

Citation: J. Chem. Phys. **139**, 084311 (2013); doi: 10.1063/1.4819062
View online: http://dx.doi.org/10.1063/1.4819062
View Table of Contents: http://jcp.aip.org/resource/1/JCPSA6/v139/i8
Published by the AIP Publishing LLC.

Quantum effects in the capture of charged particles by dipolar polarizable symmetric top molecules. I. General axially nonadiabatic channel treatment

M. Auzinsh,[1] E. I. Dashevskaya,[2,3] I. Litvin,[3] E. E. Nikitin,[2,3] and J. Troe[3,4,a)]
[1]*Department of Physics, University of Latvia, Riga LV-1586, Latvia*
[2]*Schulich Faculty of Chemistry, Technion – Israel Institute of Technology, Haifa 32000, Israel*
[3]*Max-Planck-Institut für Biophysikalische Chemie, Am Fassberg 11, Göttingen D-37077, Germany*
[4]*Institut für Physikalische Chemie, Universität Göttingen, Tammannstrasse 6, Göttingen D-37077, Germany*

(Received 2 July 2013; accepted 7 August 2013; published online 27 August 2013)

The rate coefficients for capture of charged particles by dipolar polarizable symmetric top molecules in the quantum collision regime are calculated within an axially nonadiabatic channel approach. It uses the adiabatic approximation with respect to rotational transitions of the target within first-order charge–dipole interaction and takes into account the gyroscopic effect that decouples the intrinsic angular momentum from the collision axis. The results are valid for a wide range of collision energies (from single-wave capture to the classical limit) and dipole moments (from the Vogt–Wannier and fly-wheel to the adiabatic channel limit). © *2013 AIP Publishing LLC*. [http://dx.doi.org/10.1063/1.4819062]

I. INTRODUCTION

Quantum effects in the formation of collision complexes in molecule-molecule and molecule-ion encounters are expected to show up at low collision energies when the relative motion of the partners bears quantum character, i.e., when the de-Broglie length of the radial motion becomes comparable or larger than the characteristic length of the interaction potential, and when only a small number of partial waves contribute to the capture cross section or the rate coefficient. Normally, under these conditions, the vibrational and rotational quantum states of the partners during the collision will remain adiabatic with respect to the relative motion, such that the adiabatic channel (AC) approximation[1–7] can be used to construct AC states which are considered as mutually uncoupled. Though, at low collision energy, the latter assumption is valid for states which asymptotically are separated by not too small energy spacing, it is not valid for states that arise from a lifting of the degeneracy of the rotational states with respect to the projection of the intrinsic angular momentum onto a space-fixed axis. Nonetheless, the AC approximation can be used, when the interfragment distances R, that are essential for a particular collision dynamics, are smaller than the so-called locking distance R_L, at which the quantization axis of the intrinsic angular momentum changes from space-fixed to the collision-axis direction. The locking phenomenon is well documented in the physics of atomic collisions (see, e.g., Ref. 8), and it was discussed, for molecular collisions and half-collisions, e.g., in the decay of molecular complexes in Refs. 9–12. In an application to the dynamics of complex formation, the AC approach is applicable when the characteristic capture distance is noticeably smaller than R_L. This is the case when the anisotropic interfragment interaction falls off with R faster than the Coriolis interaction (which is proportional to R^{-2}). If the former decreases more slowly then the capture is accompanied by non-adiabatic transitions between the AC states that leads to a complicated capture dynamics such as illustrated before for charge-quadrupole[13] and resonance dipole–dipole[14] interactions.

In an attempt to generalize the AC approach to cases where the Coriolis interaction is of importance, an axially nonadiabatic channel (ANC) approach was formulated in Refs. 15–17. Within this approach, the channel states and potentials were calculated by diagonalization of the sum of the interaction potential and the Coriolis coupling. This procedure eliminates the rotational nonadiabaticity (compared to the AC states and potentials), but it introduces an additional coupling induced by the radial motion. The successful application of the ANC approach is subject to certain criteria arising from the comparison of the radial and rotational coupling within the AC approach with the radial coupling within the ANC approach.[18] In this respect, the anisotropic first-order charge–dipole interaction between an ion and a dipolar symmetric top represents an interesting special case, since here the ANC states are not coupled by the radial motion. This substantially simplifies the problem of quantum capture, reducing it to two independent steps: the determination of ANC potentials and the calculation of capture probabilities from uncoupled radial wave equations. The aim of the present paper is to study such quantum effects in the capture of dipolar polarizable symmetric top molecules by ions within the ANC approach and bridge the gap between earlier studies of the problem in the classical AC (ACCl)[19–21] and the fly-wheel (FW)[22] approaches that are applicable for prevailing electrostatic or gyroscopic interactions, respectively,

When the characteristic value of the total angular momentum of the capture event is not too large for the case of first-order charge–dipole interaction, quantum effects in the capture should be accompanied by noticeable rotationally nonadiabatic effects.[22] This is the case for tops with very

a)Email: shoff@gwdg.de

small dipole moments such as arising when one of the atoms in a spherical top is isotopically substituted and when individual vibrationally averaged dipole moments of different bonds do not mutually cancel. For instance, the dipole moment of CH_3D molecule in the ground vibrational state is about 10^{-3}D[23–26] which suggests the existence of different capture regimes.[22] Here we extend this study and consider three different collision regimes, ultra-low (UL), low (L), and medium (M) energies (or temperatures), all of them falling into a range where the adiabatic approximation for rotational transitions is applicable. Still higher energies, where the adiabatic approximation and the weak-field approximation for the charge–dipole interaction break down, are not discussed here; these were considered earlier for classical relative motion.[27]

The plan of the present paper is the following. In Sec. II, ANC potentials are defined for a system ion + dipolar polarizable symmetric top, and the hierarchy of approximations is elaborated. Section III presents the capture equations and defines capture probabilities and energy-dependent rate coefficients. Section IV is devoted to ANC rate coefficients at UL energies. Section V bridges the gap between UL and M energies. Section VI concludes the paper. Paper II[36] of this series discusses energy- and temperature- dependent rate coefficients for an extended set of parameters and, as a case study, considers the capture of CH_3D by various ions.

II. HIERARCHY OF CHANNEL POTENTIALS

Following earlier work on the collision of ions and dipolar polarizable symmetric top molecules,[19–21] we consider the regime where the angular momentum of the top j and its projection k onto its symmetry axis are good quantum numbers, i.e., the "weak-field limit"[19] where the adiabatic criterion for the coupling between non-degenerate molecular states is automatically fulfilled.[20] In this case, the Hamiltonian of the collision pair, written in the total angular momentum representation (quantum number J), is diagonal in the quantum numbers J, j and reads

$$\begin{aligned} \hat{H} &= \hat{T}_R + \hat{V}, \\ \hat{V} &= \hat{H}_{\rm rot} + \hat{H}_{\rm cd} + \hat{H}_{\rm cind}. \end{aligned} \tag{2.1}$$

Here, $\hat{T}_R$ is the kinetic energy of the relative radial motion and $\hat{V}$ is the effective potential energy that includes the Hamiltonian of the relative rotation $\hat{H}_{\rm rot}$, the first-order charge–dipole interaction $\hat{H}_{\rm cd}$, and the charge–induced dipole interaction $\hat{H}_{\rm cind}$:

$$\hat{H}_{\rm rot} = \frac{(\hat{\mathbf{J}} - \hat{\mathbf{j}})^2}{2\mu R^2}, \quad \hat{H}_{\rm cd} = \frac{q\mu_D k \hat{\mathbf{j}}\mathbf{R}}{j(j+1)R^3}, \quad \hat{H}_{\rm cind} = -\frac{q^2\alpha}{2R^4}, \tag{2.2}$$

where R denotes the distance between the ion and the neutral, μ is the reduced mass of the collision pair, q is charge of the ion, μ_D is the dipole moment of the top, and α is the polarizability of the neutral molecule. Since j and k are conserved quantities, it appears practical to employ the quantity $\bar{\mu}_D = \mu_D k/\sqrt{j(j+1)}$, i.e., the projection of the molecular dipole moment onto the symmetry axis of the top in a j, k rotational state. We also note that second-order effects in the charge–dipole interaction, arising from small admixtures of other rotational states to the j, k state, can be taken into account by renormalization of the polarizability, making it j, k dependent.[18–21] However, here we will not dwell on this point.

In what follows, it is convenient to use the scaled, reduced, variables δ for the dipole moment, ρ for the interfragment separation, υ for the potentials, ε for the energy, and κ for the wave vector. These quantities are explicitly defined as

$$\begin{aligned} &\delta = q\mu\bar{\mu}_D/\hbar^2, \\ &\rho = R/R_L \quad \text{with} \quad R_L = q\sqrt{\mu\alpha}/\hbar, \\ &\upsilon = V/E_L \quad \text{with} \quad E_L = \hbar^2/\mu R_L^2 = \hbar^4/\mu^2 q^2 \alpha, \\ &\varepsilon = E/E_L = \kappa^2/2. \end{aligned} \tag{2.3}$$

In this way, the J, j block of the operator $\hat{\upsilon}$, $\hat{\upsilon}^{(J,j)}$, can be written as

$$\hat{\upsilon}^{(J,j)}(\rho, \delta) = \frac{\hat{C}^{(J,j)}(\delta)}{2\rho^2} - \frac{1}{2\rho^4}, \tag{2.4}$$

with the operator, $\hat{C}^{(J,j)}(\delta)$ given by

$$\hat{C}^{(J,j)}(\delta) = (\hat{\mathbf{J}} - \hat{\mathbf{j}})^2 + 2\delta\hat{\mathbf{j}}\boldsymbol{\rho}/\rho\sqrt{j(j+1)}. \tag{2.5}$$

If $\boldsymbol{\rho}$ is chosen as the quantization axis for $\mathbf{j}$, the matrix $\mathbf{C}^{(J,j)}$in the (J, j, m) representation, with m being the quantum number of projection of $\mathbf{j}$ onto the collision axis, reads

$$\begin{aligned} C^{(J,j)}_{m,m}(\delta) &= (J(J+1) - 2m^2 + j(j+1)) + 2\delta m/\sqrt{j(j+1)} \\ C^{(J,j)}_{m,m+1} &= C^{(J,j)}_{m+1,m} \\ &= \sqrt{J(J+1) - m(m+1)}\sqrt{j(j+1) - m(m+1)}. \end{aligned} \tag{2.6}$$

The dimensionality of the matrix $\mathbf{C}^{(J,j)}$ is $2\min(J, j) + 1$, and its eigenvalues ${}^{\rm ANC}c_n^{(J,j)}(\delta)$ can be specified, in increasing order, by a set n of numbers increasing from $-\min\{J, j\}$ up to $\min\{J, j\}$. Written in terms of eigenvalues ${}^{\rm ANC}c_n^{(J,j)}(\delta)$, the matrix $\hat{\upsilon}^{(J,j)}$ becomes diagonal with the elements

$$\upsilon_n^{(J,j)}(\rho, \delta) = \frac{{}^{\rm ANC}c_n^{(J,j)}}{2\rho^2} - \frac{1}{2\rho^4}. \tag{2.7}$$

Negative eigenvalues ${}^{\rm ANC}c_n^{(J,j)}(\delta)$ correspond to attractive ANC potentials while positive values are asymptotically repulsive potentials. If the parameter δ in the matrix $\mathbf{C}^{(J,j)}$ is replaced by $-\delta$ (which corresponds to a change of the sign of k), the set of eigenvalues will be the same, and with a proper combination of the eigenvectors for δ and $-\delta$ one gets eigenfunctions that are specified by $|\delta|$ and possess total parity P with respect to inversion of $\boldsymbol{\rho}$ and the state of the top. In the adopted approximation, when K-doubling effects are ignored, an ANC state corresponding to a certain value ${}^{\rm ANC}c_n^{(J,j)}(\delta)$ can be regarded as doubly degenerate with respect to the parity quantum numbers.

There exists a hierarchy of approximations which allows one to represent the quantities ${}^{\rm ANC}c_n^{(J,j)}(\delta)$ analytically and check these approximations by comparison with numerical results:

(i) The FW approximation: small δ, $\delta \ll 1$, arbitrary J, j. The eigenvalues ${}^{\rm ANC}c_n^{(J,j)}(\delta)$ can be calculated by perturbation approach in the (J, j, ℓ) representation with respect to δ as

$$ {}^{\rm ANC}c_n^{(J,j)}(\delta)\big|_{\delta\ll 1} \to {}^{\rm FW}\, c_\ell^{(J,j)}(\delta) = \ell(\ell+1) + O(\delta^2) + ... \tag{2.8}$$

Here, ℓ is the quantum number of the relative angular momentum with $|J-j| \le \ell \le J+j$. For the special case $J = j = -n$ (i.e., for $\ell = 0$), a series representation of ${}^{\rm FW}c_\ell^{(j,j)}(\delta)$ up to fourth order was developed in Ref. 22. It indicated an only very weak dependence of ${}^{\rm FW}c_\ell^{(j,j)}(\delta)$ on j.

(ii) The adiabatic channel (AC) approximation: large δ, $\delta \gg Jj$, arbitrary J, j. The eigenvalues ${}^{\rm ANC}c_n^{(J,j)}(\delta)$ are identified with the diagonal elements of the matrix $\mathbf{C}^{(J,j)}$ yielding

$$ {}^{\rm ANC}c_n^{(J,j)}(\delta)\big|_{\delta\gg Jj} \to {}^{\rm AC}c_n^{(J,j)}(\delta) = J(J+1) - 2n^2 + j(j+1) + 2\delta n/\sqrt{j(j+1)}. \tag{2.9}$$

The FW limit at $\delta \to 0$ and the AC limit at $\delta \gg Jj$ can be used for constructing linear correlation diagrams for the ${}^{\rm ANC}c_n^{(J,j)}(\delta)$ (i.e., the two limits connected by a straight line) obeying the non-crossing rule. As an example, Fig. 1 compares linear correlations (dashed green lines) with accurate ANC potentials (full red lines) for $j = 1$, $J = 3$.

(iii) The semiclassical ANC (ANCSC) approximation: arbitrary δ, $J \gg j$. One neglects $j(j+1)$ compared to $J(J+1)$ and approximates $\hat{C}^{(J,j)}(\delta)$ by ${}^{\rm SC}\hat{C}^{(J,j)}(\delta)$ with

$$ {}^{\rm SC}\hat{C}^{(J,j)}(\delta) = \hat{\mathbf{J}}^2 - 2\hat{\mathbf{J}}\hat{\mathbf{j}} + 2\delta\hat{\mathbf{j}}\boldsymbol{\rho}/\rho\sqrt{j(j+1)}. \tag{2.10}$$

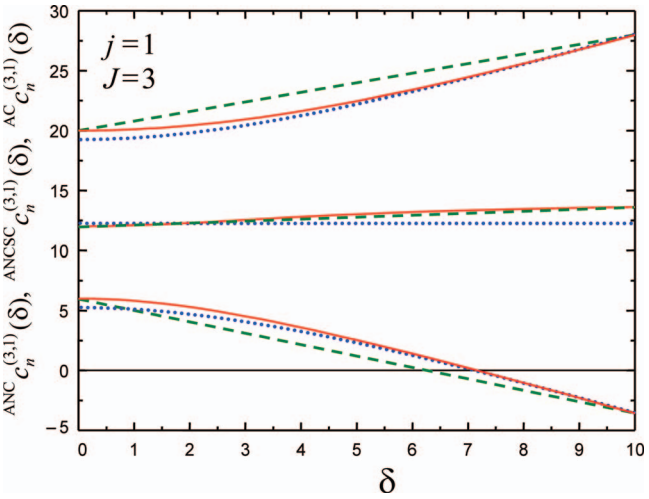

FIG. 1. Coefficients of channel potentials, see Eq. (2.7). Comparison of results for $j = 1, J = 3$ in the FW-AC linear correlation diagram ${}^{\rm FW-AC}c_n^{(3,1)}(\delta)$ (dashed green lines), ANCSC approximation ${}^{\rm ANCSC}c_n^{(3,1)}(\delta)$ (dotted blue lines), and ANC accurate results ${}^{\rm ANC}c_n^{(3,1)}(\delta)$ (full red lines); $n = -1$, 0, 1 in upward direction, δ = scaled dipole moments of Eq. (2.3)).

In addition, one considers $\hat{\mathbf{J}}$ as a classical vector which is approximately normal to $\boldsymbol{\rho}$, and one chooses the quantization axis of $\hat{\mathbf{j}}$ to coincide with the vector $\mathbf{J} + 2\delta\rho/R\sqrt{j(j+1)}$. Keeping the same nomenclature for the projection of $\mathbf{j}$ onto the new quantization axis, the matrix ${}^{\rm SC}\mathbf{C}^{(J,j)}$ becomes diagonal in this representation. Finally, replacing $J(J+1)$ by its WKB counterpart $(J+1/2)^2$, one gets

$$ {}^{\rm ANC}c_n^{(J,j)}(\delta)\big|_{J\gg j} \to {}^{\rm ANCSC}c_n^{(J,j)}(\delta) = (J+1/2)^2 + n\sqrt{(2J+1)^2 + 4\delta^2/j(j+1)}. \tag{2.11}$$

Fig. 1 illustrates the performance of the ANCSC approximation for $J = 3$, $j = 1$when the condition $J \gg j$ is nearly satisfied (dotted blue lines).

(iv) The AC classical (ACCl) approximation: large δ, $\delta \gg Jj$, arbitrary j, $J \gg j$, 1. Here, in Eq. (2.9) for ${}^{\rm AC}c_n^{(J,j)}(\delta)$, one assumes $J \gg j$, neglects n^2 and $j(j+1)$ against J^2 and replaces $J(J+1)$ by $(J+1/2)^2$. This yields

$$ {}^{\rm ANC}c_n^{(J,j)}(\delta)\big|_{\delta\gg Jj, J\gg j} \to {}^{\rm ACCl}c_n^{(J,j)}(\delta) = (J+1/2)^2 + 2\delta n/\sqrt{j(j+1)}. \tag{2.12}$$

This is the standard expression of the ACCl approximation which was used in earlier work for calculating capture rate coefficients at moderate collision energies.[19–21]

(v) We finally note that, for $j = 1$ and $j = 2$, the functions $\delta(c_n^{(J,1)})$ that are inverse to $c_n^{(J,1)}(\delta)$, can be calculated analytically. In particular, for $j = 1$, the result reads

$$ \delta = \frac{\left|J(J+1) - c_n^{(J,1)}\right|}{\sqrt{2}} \times \sqrt{1 - 4\frac{J(J+1)}{\left(J(J+1) - c_n^{(J,1)}\right)\left(J(J+1) + 2 - c_n^{(J,1)}\right)}}, \tag{2.13}$$

where n assumes the values $n = -1$, 0, and1 (see Sec. IV).

III. CAPTURE EQUATIONS, CROSS SECTIONS, AND RATE COEFFICIENTS

Since the diagonalization of the $\mathbf{C}^{(J,j)}$ matrix removes the rotational (Coriolis) coupling, and since this diagonalization is performed by an ρ-independent transformation, the ANC potentials of Eq. (2.7) play the part of ordinary central potentials, i.e., the multi-state Hamiltonian of Eq. (2.4) becomes a set of single-state Hamiltonians with the ANC potentials

$$ \left\{-\frac{\partial^2}{2\partial\rho^2} + \upsilon_n^{(J,j)}(\rho,\delta)\right\}\psi_n^{(J,j)}(\rho,\kappa) = \varepsilon\psi_n^{(J,j)}(\rho,\kappa), \tag{3.1}$$

where ε and κ are from Eq. (2.3). The solutions of Eq. (3.1), with appropriate capture boundary conditions,[21] determine the capture probabilities $P_n^{(J,j)}(\kappa,\delta)$. These are

recovered from the capture probability $P(\kappa, c)$ calculated for a Hamiltonian $\hat{\eta}(\rho, c)$,

$$\hat{\eta}(\rho, c) = -\frac{d^2}{2d\rho^2} + \upsilon(\rho, c), \qquad \upsilon(\rho, c) = \frac{c}{2\rho^2} - \frac{1}{2\rho^4}, \tag{3.2}$$

as

$$P_n^{(J,j)}(\kappa, \delta) = P(\kappa, c)\big|_{c=c_n^{(J,j)}(\delta)}. \tag{3.3}$$

For $c > 0$, the potential $\upsilon(\rho, c)$in Eq. (3.2) reaches its maximum $\upsilon_{\max}(c) = c^2/8$ at an energy ε_c corresponding to $\kappa_c = c/2$. For $c < 0$, the potential is purely attractive.

Equation (3.2) can be solved with Mathieu functions.[28–31] However, in the following we adhere to numerical solutions which either are directly put into the expressions for the rate coefficients or provide the basis for relatively simple analytical fitting formulae (see Sec. V).

The probabilities $P_n^{(J,j)}(\kappa, \delta)$ determine the total cumulative capture probability $\Pi^{(j)}(\kappa, \delta)$,

$$\Pi^{(j)}(\kappa, \delta) = \sum_{J,n} \frac{2J+1}{2j+1} {}^{\mathrm{ANC}}P_n^{(J,j)}(\kappa, \delta), \tag{3.4}$$

and the total rate coefficients. The latter, scaled relative to the energy-independent Langevin rate coefficient $k_{\mathrm{Lang}} = 2\pi q\sqrt{\alpha/\mu}$, are

$${}^{\mathrm{ANC}}\chi^{(j)}(\kappa, \delta) = \frac{1}{2\kappa} {}^{\mathrm{ANC}}\Pi^{(j)}(\kappa, \delta). \tag{3.5}$$

The ANCSC and AC counterparts of Eqs. (3.4) and (3.5) are obtained from these equations when the ANC probabilities in Eq. (3.4) are replaced by AC and ANCSC probabilities. The ACCl counterpart is obtained from Eq. (3.5) when the probabilities are expressed by steps of the energy at the barriers of the effective potentials in the Hamiltonian in Eq. (3.3) and when the summation over J is replaced by an integration (see Sec. IV for more details).

ANC thermal capture rate coefficients are obtained by averaging of the energy-dependent capture rate coefficients. The averaged scaled capture rate coefficient, averaged scaled capture rate coefficient ${}^{\mathrm{ANC}}\bar{\chi}^{(j)}(\theta, \delta)$, are expressed as a function of the scaled temperature $\theta = k_{\mathrm{B}}T/E_L$ where E_L is defined by Eq. (2.3) (see Paper II[36]).

IV. QUANTUM ANC CAPTURE AT ULTRA-LOW ENERGIES

The regime of UL collision energies is defined by the condition that, in the absence of a charge–dipole interaction, the rate coefficient is dominated by s-wave capture. Quantitatively, we define this region by the condition $\kappa < 0.1$ which corresponds to collision energies below the classical barrier height $c_{\mathrm{UL}}^2/8$ of the potential in Eq. (3.2) and $c_{\mathrm{UL}} = 0.2$ (we note that this value of c is an order of magnitude lower than the respective value for p-wave capture, $c_p = 2$). Indeed, Fig. 1 of Ref. 32 shows that the probability of p-wave capture at $\kappa = 0.1$ is about two orders of magnitude smaller than that for s-wave capture.

For not too small values of δ, we expect that rate coefficients at UL energies will be determined by the long-range part of the interaction potential only and, therefore, will not be too different from that for pure charge–dipole (CD) interaction. We, therefore, first consider, capture for pure CD interaction. For this case, an attractive interaction corresponds to $c_n^{(J,j)}(\delta) < 0$ which is possible only for negative values of n. The capture probabilities in this case are step functions Θ of the coefficients $c_n^{(J,j)}(\delta)$ where the step corresponding to the opening of the capture channel at $c_n^{(J,j)}(\delta) = -1/4$ determines the onset of capture for a pure R^{-2} attraction (see Sec. 35 of Ref. 33). Thus we have

$$\begin{aligned} {}^{\mathrm{ANCCD}}\chi^{(j)}(\kappa, \delta) &= \frac{1}{2\kappa} {}^{\mathrm{ANCCD}}N^{(j)}(\delta), \\ {}^{\mathrm{ANCCD}}N^{(j)}(\delta) &= \sum_{J,n} \frac{2J+1}{2j+1} \Theta\left(-1/4 - c_n^{(J,j)}(\delta)\right), \end{aligned} \tag{4.1}$$

where ${}^{\mathrm{ANCCD}}N^{(j)}(\delta)$ is the mean ANC number of open CD channels. The steps ${}^{\mathrm{ANCCD}}N^{(j)}(\delta)$ increase by $(2J+1)/(2j+1)$ each time when δ passes a threshold value ${}^{\mathrm{ANC}}\delta_n^{(J,j)}$. The latter are found from the equation,

$${}^{\mathrm{ANC}}c_n^{(J,j)}(\delta)\big|_{\delta={}^{\mathrm{ANC}}\delta_n^{(J,j)}} = -1/4, \tag{4.2}$$

which has a solution only for negative n. The values of ${}^{\mathrm{ANC}}\delta_n^{(J,j)}$ are listed in Table I for (J, j, n) triads which are of interest for capture at UL energies. The ACCD counterpart of ${}^{\mathrm{ANCCD}}N^{(j)}(\delta)$, i.e., ${}^{\mathrm{ACCD}}N^{(j)}(\delta)$, is obtained when the ${}^{\mathrm{ANC}}\delta_n^{(J,j)}$ in Eq. (4.1) are replaced by ${}^{\mathrm{AC}}\delta_n^{(J,j)}$ from the equivalent of Eq. (4.2). The values of ${}^{\mathrm{AC}}\delta_n^{(J,j)}$ are found analytically from Eq. (2.9). The comparison of ${}^{\mathrm{ANC}}\delta_n^{(J,j)}$ with ${}^{\mathrm{AC}}\delta_n^{(J,j)}$(see Table I) demonstrates the importance of the gyroscopic

TABLE I. Threshold values ${}^{\mathrm{ANC}}\delta_n^{(J,j)}$ (upper lines) and ${}^{\mathrm{AC}}\delta_n^{(J,j)}$ (lower lines) for $j = 1$, 2, and 3 and $J = 1$, 2, 3, and 4. The first thresholds ${}^{\mathrm{ANC}}\delta_{-j}^{(j,j)}$ and ${}^{\mathrm{AC}}\delta_{-j}^{(j,j)}$ are in bold.

j	n	$J = 1$ ANC, AC	$J = 2$ ANC, AC	$J = 3$ ANC, AC	$J = 4$ ANC, AC
1	−1	**0.643, 1.59**	3.23, 4.42	7.38, 8.66	13.00, 14.32
2	−1	5.60, 7.65	9.88, 12.55	17.09, 19.90	26.90, 29.70
	−2	None	**0.641, 2.60**	3.34, 6.28	7.66, 11.18
3	−1	18.07, 21.22	24.17, 28.15	34.18, 38.54	47.95, 52.40
	−2	None	4.72, 8.88	8.49, 14.07	14.72, 21.00
	−3	None	None	**0.640, 3.61**	3.42, 8.23

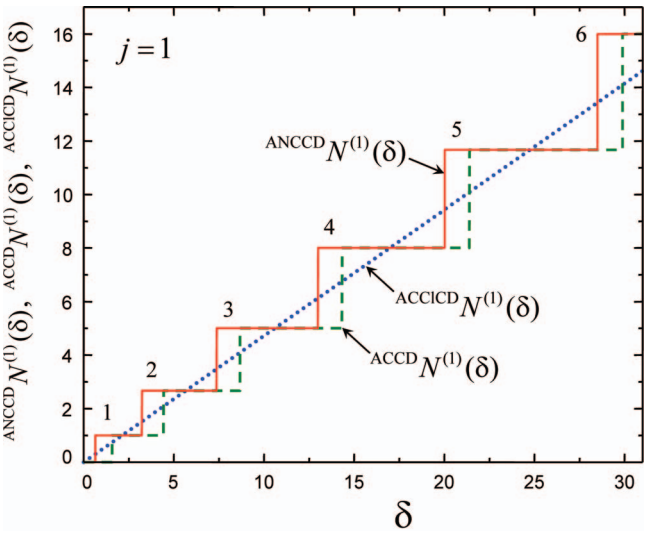

FIG. 2. Total number ${}^{\mathrm{ANCCD}}N^{(j)}(\delta)$ of ANCCD (red full line), ${}^{\mathrm{ACCD}}N^{(j)}(\delta)$ of ACCD (green dashed line), and ${}^{\mathrm{ACClCD}}N^{(j)}(\delta)$ of ACClCD (dotted blue line) capture states for $j = 1$. (In this case there is only one capture state for each J with $n = -1$; the given numbers are maximum values of contributing J; δ = scaled dipole moments of Eq. (2.3).)

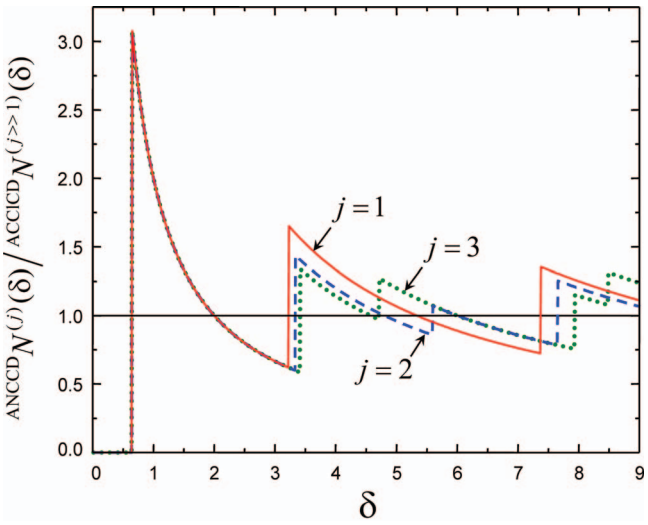

FIG. 3. Dependence of the ratio ${}^{\mathrm{ANCCD}}N^{(j)}(\delta)/{}^{\mathrm{ACClCD}}N^{(j\gg1)}(\delta)$ on δ for $j = 1$ (red full line), $j = 2$ (blue dashed line), $j = 3$ (green dotted line), see Fig. 2.

effect for δ being between ${}^{\mathrm{ANC}}\delta_n^{(J,j)}$ and ${}^{\mathrm{AC}}\delta_n^{(J,j)}$. Finally, ${}^{\mathrm{ACClCD}}\chi^{(j)}(\kappa,\delta)$ and ${}^{\mathrm{ACClCD}}N^{(j)}(\delta)$ are calculated from Eq. (4.1) when the ${}^{\mathrm{ANC}}\delta_n^{(J,j)}$ are replaced by ${}^{\mathrm{ACCl}}\delta_n^{(J,j)}$ and the summation by an integration,

$$
\begin{aligned}
{}^{\mathrm{ACClCD}}\chi^{(j)}(\kappa,\delta) &= \frac{1}{2\kappa}\,{}^{\mathrm{ACClCD}}N^{(j)}(\delta),\\
{}^{\mathrm{ACClCD}}N^{(j)}(\delta) &= \delta\frac{\sqrt{j(j+1)}}{(2j+1)}.
\end{aligned}
\tag{4.3}
$$

Fig. 2 illustrates the relation between ${}^{\mathrm{ANCCD}}N^{(j)}(\delta)$, ${}^{\mathrm{ACCD}}N^{(j)}(\delta)$, and ${}^{\mathrm{ACClCD}}N^{(j)}(\delta)$ for $j = 1$. Here exists only one contribution with $n = -1$, and ${}^{\mathrm{ANCCD}}N^{(1)}(\delta)$ is a function with regular steps of progressively increasing length.

For $j = 2$, there are two contributions with $n = -2$ and $n = -1$, and ${}^{\mathrm{ANCCD}}N^{(2)}(\delta)$ is the sum of them. As a result, ${}^{\mathrm{ANCCD}}N^{(2)}(\delta)$ has the shape of a slightly irregular step function. For $j = 3$, i.e., for ${}^{\mathrm{ANCCD}}N^{(3)}(\delta)$, the irregularity in ${}^{\mathrm{ANCCD}}N^{(3)}(\delta)$ increases further since there are three contributions from $n = -3$, $n = -2$, and $n = -1$. These patterns are summarized in Fig. 3 for $j = 1$, 2, and 3 and they are illustrated by the ratios of capture rate coefficients,

$$
{}^{\mathrm{ANCCD}}S^{(j)}(\delta) = \frac{{}^{\mathrm{ANCCD}}\chi^{(j)}_{\mathrm{app}}(\kappa,\delta)}{{}^{\mathrm{ACClCD}}\chi^{(j)}(\kappa,\delta)} = \frac{{}^{\mathrm{ANCCD}}N^{(j)}(\delta)}{{}^{\mathrm{ACClCD}}N^{(j)}(\delta)}. \tag{4.4}
$$

The peaks of the plots ${}^{\mathrm{ANCCD}}S^{(j)}(\delta)$ correspond to the threshold values ${}^{\mathrm{ANC}}\delta_n^{(J,j)}$ which, in increasing order, are ${}^{\mathrm{ANC}}\delta_{-1}^{(1,1)} \approx {}^{\mathrm{ANC}}\delta_{-2}^{(2,2)} \approx {}^{\mathrm{ANC}}\delta_{-3}^{(3,3)}$, ${}^{\mathrm{ANC}}\delta_{-1}^{(2,1)}$, ${}^{\mathrm{ANC}}\delta_{-2}^{(3,2)}$, ${}^{\mathrm{ANC}}\delta_{-3}^{(4,3)}$, ${}^{\mathrm{ANC}}\delta_{-2}^{(4,3)}$, ${}^{\mathrm{ANC}}\delta_{-1}^{(3,2)}$, ${}^{\mathrm{ANC}}\delta_{-1}^{(3,1)}$, ${}^{\mathrm{ANC}}\delta_{-2}^{(4,2)}$, ${}^{\mathrm{ANC}}\delta_{-3}^{(5,3)}$, ${}^{\mathrm{ANC}}\delta_{-3}^{(6,3)}$. With increasing δ, the sawtooth shaped ratios ${}^{\mathrm{ANCCD}}N^{(j)}(\delta)/{}^{\mathrm{ACClCD}}N^{(j)}(\delta)$ with jumps at $\delta = {}^{\mathrm{ANC}}_{t}\delta_n^{(J,j)}$ converge to unity. Since the increments of ${}^{\mathrm{ANCCD}}N^{(j)}(\delta)$ at each large step are proportional to $\sqrt{\delta}$, and since ${}^{\mathrm{ACClCD}}N^{(j)}(\delta)$ increases linearly with δ, the individual deviations of the ratio ${}^{\mathrm{ANCCD}}N^{(j)}(\delta)/{}^{\mathrm{ACClCD}}N^{(j)}(\delta)$ from unity decrease as $1/\sqrt{\delta}$, i.e., relatively slowly. The plots of ${}^{\mathrm{ANCCD}}S^{(j)}(\delta)$ show that, for some values of δ, to the right from ${}^{\mathrm{ANC}}\delta_n^{(J,j)}$, the ratio ${}^{\mathrm{ANCCD}}S^{(j)}(\delta)$, in its decreasing parts, becomes equal to unity (i.e., the ${}^{\mathrm{ANCCD}}N^{(j)}(\delta)$ become equal or close to ${}^{\mathrm{ANCCD}}N^{(j\gg1)}(\delta)$). We call these values the reference values ${}^{\mathrm{R}}\delta_n^{(J,j)}$. The set of ${}^{\mathrm{ANC}}\delta_n^{(J,j)}$ and ${}^{\mathrm{R}}\delta_n^{(J,j)}$ qualitatively characterize the δ dependence of ${}^{\mathrm{ANCCD}}S^{(j)}(\delta)$.

Passing to the general case (charge–dipole + charge–induced dipole interactions), we suggest an approximation to the case when several capture channels are open in the UL energy region. Explicitly, we accept the following expression for the approximate rate coefficient (denoted by ${}^{\mathrm{ANCUL}}\chi^{(j)}(\kappa,\delta)$) which includes contributions only from ${}^{\mathrm{ANC}}c_n^{(J,j)}(\delta)$ with $n < 0$ and uses approximate capture probabilities $P^{(J,j)}_{n,\mathrm{app}}(\kappa,\delta)$ instead of the accurate $P_n^{(J,j)}(\kappa,\delta)$:

$$
\begin{aligned}
{}^{\mathrm{ANCUL}}\chi^{(j)}(\kappa,\delta) &\approx {}^{\mathrm{ANCUL}}\chi^{(j)}_{\mathrm{app}}(\kappa,\delta) = \frac{1}{2\kappa}\,{}^{\mathrm{ANCUL}}\Pi^{(j)}_{\mathrm{app}}(\kappa,\delta),\\
{}^{\mathrm{ANCUL}}\Pi^{(j)}_{\mathrm{app}}(\kappa,\delta) &= \sum_{J,n}\frac{2J+1}{2j+1}\,{}^{\mathrm{ANC}}P^{(J,j)}_{n,\mathrm{app}}(\kappa,\delta).
\end{aligned}
\tag{4.5}
$$

The validity of this approximation is determined by the condition that the partial contributions from terms with ${}^{\mathrm{ANC}}c_n^{(J,j)}(\delta) > c_{\mathrm{UL}}$ in the general expression of Eq. (3.4) are negligible compared to UL rate coefficients, and the approximate probabilities $P^{(J,j)}_{n,\mathrm{app}}(\kappa,\delta)$ well reproduce the accurate probabilities $P_n^{(J,j)}(\kappa,\delta)$ in the regions which are essential for the sum in Eq. (4.5).

The approximation of $P_n^{(J,j)}(\kappa,\delta)$ by $P^{(J,j)}_{n,\mathrm{app}}(\kappa,\delta)$ relies on the behavior of $P(\kappa, c)$ at small κ which shows a steep drop as a function of c in the range $-1 < c < 1$, see Fig. 4.

Interestingly, capture channels for charge–dipole + charge–induced dipole interaction at very small κ open up at larger negative c than for pure CD interaction, where $c = -1/4$ (vertical line in Fig. 4). This is related to the reflection of the waves above the drop of the $-1/\rho^4$ potential. The desired approximate expression for the probabilities

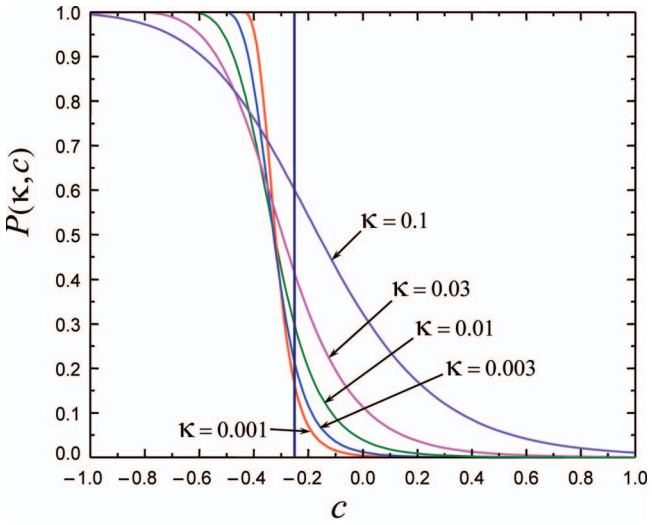

FIG. 4. Capture probabilities $P(\kappa, c)$ over the range $-1 < c < 1$ (κ = scaled wave vector from Eq. (2.3), c = scaled potential parameter from Eq. (3.2)).

${}^{\mathrm{ANC}}P^{(J,j)}_{n,\mathrm{app}}(\kappa, \delta)$ is obtained in two steps: the first replaces $P(\kappa, c)$ by $P_{\mathrm{app}}(\kappa, c)$, and the second replaces ${}^{\mathrm{ANC}}c^{(J,j)}_{n}(\delta)$ by ${}^{\mathrm{ANC}}c^{(J,j)}_{n,\mathrm{app}}(\delta)$, i.e.,

$$ {}^{\mathrm{ANC}}P^{(J,j)}_{n,\mathrm{app}}(\kappa, \delta) = P_{\mathrm{app}}(\kappa, c)\big|_{c={}^{\mathrm{ANC}}c^{(J,j)}_{n,\mathrm{app}}(\delta)}. \tag{4.6}$$

Our approximation for $P_{\mathrm{app}}(\kappa, c)$ is based on the fitting of numerical probabilities $P(\kappa, c)$ in terms of sigmoid functions of the form

$$ P_{\mathrm{app}}(\kappa, c) = \frac{1}{1 + \exp[\alpha_c(c - c_{1/2})]}. \tag{4.7}$$

Here, $c_{1/2} = c_{1/2}(\kappa)$ fixes the center of the sigmoid that corresponds to $P_{\mathrm{app}}(\kappa, c)|_{c_{1/2}=c_{1/2}(\kappa)} = 1/2$, and $\alpha_c(\kappa) = \alpha_>(\kappa) \mathrm{or} \alpha_<(\kappa)$ characterizes the half-width of the sigmoid for $c > c_{1/2}$ and $c < c_{1/2}$, respectively. The fitted functions $c_{1/2}(\kappa)$ and $\alpha_c(\kappa)$, expressed through the auxiliary variable $\xi = \lg\left(10^3\kappa\right)$, have the form

$$\begin{aligned} c_{1/2}(\kappa) &= -0.323 - 0.014\xi + \exp(-7.5 + 3.25\xi - 0.165\xi^2), \\ \alpha(\kappa) &= \begin{bmatrix} \alpha_<(\kappa), c < c_{1/2}(\kappa) \\ \alpha_>(\kappa), c > c_{1/2}(\kappa) \end{bmatrix}, \\ \alpha_<(\kappa) &= 6.35\xi^2 - 27.15\xi + 34, \\ \alpha_>(\kappa) &= 1.8\xi^2 - 12\xi + 21. \end{aligned} \tag{4.8}$$

For $c > -1/4$, an analytical expression for $P(\kappa, c)$ at small κ and under the condition $P(\kappa, c) \ll 1$ was derived by Fabrikant and Hotop.[34] Our numerical results agree well with their findings, but we abandon this result in order to arrive at a more global expression in the form of Eqs. (4.6) and (4.7) which describes the transition from large to small capture probabilities when c passes through the value $-1/4$. For c significantly different from $-1/4$, the approximation of Eq. (4.7) becomes inadequate, but this does not noticeably affect the partial rate coefficients since the ${}^{\mathrm{ANC}}P^{(J,j)}_{n,\mathrm{app}}(\kappa, \delta)$ become either negligibly small or flatten off to their asymptotic values of unity.

Our approximation of ${}^{\mathrm{ANC}}c^{(J,j)}_{n}(\delta)$ by ${}^{\mathrm{ANC}}c^{(J,j)}_{n,\mathrm{app}}(\delta)$ is based on a fitting of the numerical eigenvalues of the $C^{(J,j)}$ matrices in certain regions of δ. With coefficients $a^{(J,j)}_n$ such as given in Table II, for the same triads (J, j, n) as in Table I, we write

$$ {}^{\mathrm{ANC}}c^{(J,j)}_{n,\mathrm{app}}(\delta) = -1/4 + {}^{\mathrm{ANC}}a^{(J,j)}_n\left({}^{\mathrm{ANC}}\delta^{(J,j)}_n - \delta\right), \tag{4.9}$$

for all (J, j, n) triads except for $(j, j, -j)$. For the latter, that corresponds to the minimal value of ${}^{\mathrm{ANC}}\delta^{(J,j)}_n$, the approximation reads:

$$\begin{aligned} &{}^{\mathrm{ANC}}c^{(j,j)}_{-j,\mathrm{app}}(\delta) \\ &= -1/4 + a^{(j,j)}_{-j}\left({}^{\mathrm{ANC}}\delta^{(j,j)}_{-j} - \delta\right) + \frac{1/4 - a^{(j,j)}_{-j}{}^{\mathrm{ANC}}\delta^{(J,j)}_n}{\left({}^{\mathrm{ANC}}\delta^{(j,j)}_{-j}\right)^2} \\ &\quad \times\left({}^{\mathrm{ANC}}\delta^{(j,j)}_{-j} - \delta\right)^2. \end{aligned} \tag{4.10}$$

Also listed in Table II are J-independent coefficients ${}^{\mathrm{AC}}a^{(J,j)}_n = 2n/\sqrt{j(j+1)}$ which noticeably deviate from ${}^{\mathrm{ANC}}a^{(J,j)}_n$, though the latter converge slowly to the former (for J noticeably exceeding j). The linear approximation near ${}^{\mathrm{ANC}}\delta^{(J,j)}_n$ in Eq. (4.9) breaks down for those δ which strongly deviate from the threshold values ${}^{\mathrm{ANC}}\delta^{(J,j)}_n$. However, this does not noticeably affect the partial rate coefficients since ${}^{\mathrm{ANC}}P^{(J,j)}_{n,\mathrm{app}}(\kappa, c)|_{c={}^{\mathrm{ANC}}c^{(J,j)}_{n,\mathrm{app}}(\delta)}$ becomes either negligibly small or flattens off to its asymptotic values of unity for increasing values of $|{}^{\mathrm{ANC}}\delta^{(J,j)}_n - \delta|$. The linear term in Eq. (4.10) is supplemented by a quadratic term which insures the correct limit at $\delta \to 0$. This is necessary since the value ${}^{\mathrm{ANC}}c^{(J,j)}_{n}(\delta)_{\delta=0} = 0$ falls into the UL energy range. We note, however, that the approximation of Eq. (4.10), intended to provide the optimum approximation to ${}^{\mathrm{ANC}}c^{(j,j)}_{-j}(\delta)$ near the threshold $\delta = {}^{\mathrm{ANC}}\delta^{(j,j)}_{-j}$, is slightly different from the approximation of Eq. (2.9) near $\delta = 0$. In this way, Eqs. (4.9) and (4.10) as well as Tables I and II summarize the results of the diagonalization of the ANC matrices which are needed in the UL energy region.

Passing to the ANCUL rate coefficients we note that, for δ below and of the order of unity, only one term in the sum of Eq. (4.4) with $J = j = -n$ survives. Then, ${}^{\mathrm{ANCUL}}\chi^{(j)}_{\mathrm{app}}(\kappa, \delta)$

TABLE II. Expansion coefficients ${}^{\mathrm{ANC}}a^{(J,j)}_n$ (upper lines) and ${}^{\mathrm{AC}}a^{(J,j)}_n$ (lower lines) for $j = 1$, 2, and 3 and $J = 1$, 2, 3, and 4 in Eqs. (5.7) and (5.8).

j	n	$J=1$	$J=2$	$J=3$	$J=4$
1	−1	−0.712	−1.096	−1.228	−1.293
		−1.414	−1.414	−1.414	−1.414
2	−1	−0.633	−0.643	−0.697	−0.735
		−0.816	−0.816	−0.816	−0.816
	−2	None	−0.720	−1.098	−1.252
			−1.633	−1.633	−1.633
3	−1	−0.500	−0.493	−0.504	−0.522
		−0.577	−0.577	−0.577	−0.577
	−2	None	−0.777	−0.776	−0.856
			−1.155	−1.155	−1.155
	−3	None	None	−0.721	−1.082
				−1.732	−1.732

assumes the form

$$^{\mathrm{ANCUL}}\chi^{(j)}_{\mathrm{app}}(\kappa,\delta) = \frac{1}{2\kappa} P_{\mathrm{app}}\left(\kappa, {}^{\mathrm{ANC}}c^{(j,j)}_{-j,\mathrm{app}}(\delta)\right), \tag{4.11}$$

where $c^{(j,j)}_{-j,\mathrm{app}}(\delta)$ is defined by Eq. (4.10). A more accurate expression for $^{\mathrm{ANCUL}}\chi^{(j)}_{\mathrm{app}}(\kappa,\delta)$, in the limit of very small δ, in the framework of the FW approach was given in Ref. 22. In particular, for $\delta \ll 1$ and $\kappa \to 0$, the FW rate coefficients read:

$$^{\mathrm{FW}}\chi^{(j)}(\kappa,\delta)|_{\delta\ll 1,\kappa\to 0} = 2(\kappa/4)^{-4\delta^2/3}. \tag{4.12}$$

The expression of Eq. (4.11) at $\delta \to 0$ yields the Vogt-Wannier (VW) limit $^{\mathrm{FW}}\chi^{(j)}(\kappa,\delta)|_{\delta=0,\kappa\to 0} = {}^{\mathrm{VW}}\chi = 2$, though, for non-zero δ, it diverges for $\kappa \to 0$. It was argued in Ref. 22 that the condition $\delta \ll 1$, inherent in the FW approximation, can be relaxed, since, for $\delta \to 1$, the FW capture probability approaches its maximum value, thus being quite insensitive to the actual value of c. Indeed, Fig. 4 shows that the maximum is achieved with an accuracy of 5% at $c = -0.5$ for $\kappa = 0.01$ and at $c = -0.7$ for $\kappa = 0.1$. These results confirm that the quadratic approximation $c = 2\delta^2/3$ can be used for an approximate calculation of $^{\mathrm{FW}}P(\kappa,\delta)$ when $^{\mathrm{FW}}P(\kappa,\delta)$ approaches its maximal value of $^{\mathrm{FW}}_{\max}\chi(\kappa) = 1/2\kappa$.

For larger δ, several terms in the sum in Eq. (3.4) may contribute, with larger values of J explicitly containing the capture probability while the others will be at their unitary limit. When there is only a single such term, then the $^{\mathrm{ANCUL}}\chi^{(j)}_{\mathrm{app}}(\kappa,\delta)$ can be expressed as

$$^{\mathrm{ANCUL}}\chi^{(j)}_{\mathrm{app}}(\kappa,\delta) = \frac{1}{2\kappa}\left\{ {}^{\mathrm{ANCCD}}N^{(j)}(\delta) + \frac{2J_m+1}{2j+1} {}^{\mathrm{ANC}}P_{\mathrm{app}}(\kappa, c^{(J_m,j)}_{n_m,\mathrm{app}}(\delta)\right\}. \tag{4.13}$$

Here, $^{\mathrm{ANCCD}}N^{(j)}(\delta)$ is the number of ANCCD open channels with the maximum quantum number $J_m - 1$, while $J_m = J_m(\delta)$ and $n_m = n_m(\delta)$ are determined from the equation

$$\delta^{(J_m,j)}_{n_m} = \max\{\delta^{(J,j)}_n\}\big|_{\delta^{(J,j)}_n<\delta}. \tag{4.14}$$

If $J_m(\delta) = j$, then $^{\mathrm{ANCCD}}N^{(j)}(\delta) = 0$, and Eq. (4.13) reduces to Eq. (4.10). The form of Eq. (4.13) suggests that, for a fixed energy, the dependence of the capture cross section on δ is represented by a series of steps connected by sigmoid joints. The joints are quite steep for very low κ, but become broader with increasing κ. This is a manifestation of the charge–induced dipole interaction in the capture dynamics. It can be characterized by generalizing the ratio of Eq. (4.4) as

$$^{\mathrm{ANCUL}}S^{(j)}(\kappa,\delta) = \frac{^{\mathrm{ANCUL}}\chi^{(j)}(\kappa,\delta)}{^{\mathrm{ACCICD}}\chi^{(j)}(\kappa,\delta)} = \frac{^{\mathrm{ANCUL}}\Pi^{(j)}(\kappa,\delta)}{^{\mathrm{ACCICD}}N^{(j)}(\delta)}. \tag{4.15}$$

More details of the given approach can be illustrated for the case $j = 1$. Here, the quantities $^{\mathrm{ANC}}\delta^{(J,1)}_{-1}$ and $a^{(J,1)}_{-1} = (d\delta/dc)^{-1}$ at $c = -1/4$ that enter into Eqs. (4.8) and (4.9) are calculated analytically from Eq. (2.13). In particular, the threshold values $^{\mathrm{ANC}}\delta^{(J,1)}_{-1}$ are

$$^{\mathrm{ANC}}\delta^{(J,1)}_{-1} = \frac{(J+1/2)}{\sqrt{2}}\sqrt{1 - \frac{4J(J+1)}{(J+1/2)^2\left((J+1/2)^2+2\right)}}, \tag{4.16}$$

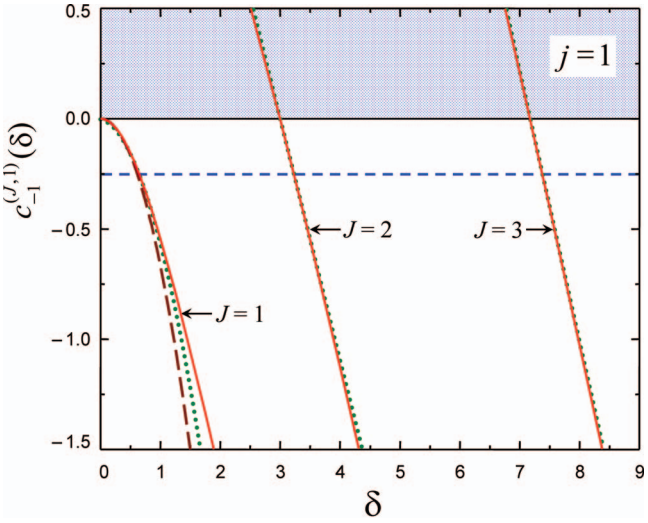

FIG. 5. Coefficients of channel potentials $^{\mathrm{ANC}}c^{(J,j)}_n(\delta)$, see Eq. (2.7), for $j = 1$, $n = -1$, and $J = 1$, 2, and 3 (red full lines) that contribute to the rate coefficients at UL energies (the crossings of $^{\mathrm{ANC}}c^{(J,1)}_{-1}(\delta)$ with the blue dashed line $^{\mathrm{ANC}}c^{(J,1)}_{-1} = -1/4$ correspond to the opening of capture channels for pure CD interaction; the green dotted lines correspond to the analytical fitting by Eqs. (4.9) and (4.10), the dashed brown line to the second-order approximation for $^{\mathrm{FW}}c^{(1,1)}_0(\delta)$ in Eq. (2.8)).

yielding the first threshold as $^{\mathrm{ANC}}\delta^{(1,1)}_{-1} = 45/4\sqrt{306} \approx 0.643$. Plots of $^{\mathrm{ANC}}\delta^{(J,1)}_{-1}$ for $J = 1$, 2, and 3 within the UL energy range ($c < 0.2$) are shown in Fig. 5 (full lines), together with the approximations from Eqs. (4.9) and (4.10) (dotted green lines). The latter, for not too small values of δ, perform noticeably better than the second-order approximation for $^{\mathrm{FW}}c^{(1,1)}_0(\delta) = 2\delta^2/3$ in Eq. (2.8) (dashed brown line).

At least up to $\delta = 2.5$, the contribution from the channel $J = 2$ is negligible compared to that from the leading channel $J = 1$, i.e., a single-term approximation for $^{\mathrm{ANCUL}}\chi^{(1)}_{\mathrm{app}}(\kappa,\delta)$ in Eq. (4.10) is valid for $\delta < 2.5$. This substantiates the suggestion from Ref. 22 that, for $\delta < 2$, one can safely use the one-channel approximation for UL conditions.

Fig. 6 compares plots of the ratios $^{\mathrm{ANCUL}}S^{(1)}(\kappa,\delta)$ over the range $0.4 < \delta < 6$ (dotted-dashed, dashed, and dotted lines for different values of κ, $\kappa = 0.1$, 0.01, and 0.001) with the plot of $^{\mathrm{ANCCD}}S^{(1)}(\delta)$ (full line). This region of δ accommodates two threshold values $^{\mathrm{ANC}}\delta^{(1,1)}_{-1}$ and $^{\mathrm{ANC}}\delta^{(2,1)}_{-1}$(corresponding to abrupt jumps of the CD curve), as well as two reference values $^{\mathrm{R}}\delta^{(1,1)}_{-1}$ and $^{\mathrm{R}}\delta^{(2,1)}_{-1}$ (corresponding to the roots of the equation $^{\mathrm{ANCCD}}S^{(1)}(\delta) = 1$).

One sees the noticeable shifts of the maxima of the sigmoids $^{\mathrm{ANCUL}}S^{(1)}(\kappa,\delta)$ with respect to the CD threshold positions $\delta = {}^{\mathrm{ANC}}\delta^{(J,1)}_1$, ($J = 1$ and 2), and the approximate fulfillment of the relation $^{\mathrm{ANCUL}}S^{(1)}(\kappa, {}^{\mathrm{R}}\delta^{(J,1)}_{-1}) = 1$ ($J = 1$ and 2). The former feature is a direct consequence of the sigmoid shape of $P(\kappa, c)$ in Fig. 4, while the latter will be discussed in Sec. V. Finally we note that plots of $^{\mathrm{ANCUL}}S^{(1)}(\kappa,\delta)$ for $\delta < 0.4$ can be constructed by replacing $^{\mathrm{ANCUL}}\chi^{(j)}(\kappa,\delta)$ by $\chi^{\mathrm{FW}}(\kappa,\delta)$, with the latter given by analytical expressions and Fig. 1 of Ref. 22.

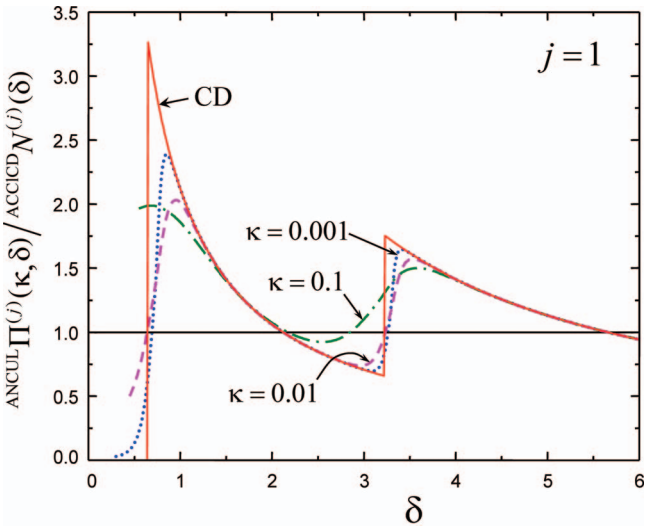

FIG. 6. Ratios ${}^{\mathrm{ANCUL}}\Pi^{(j)}(\kappa, \delta)/{}^{\mathrm{ACClCD}}N^{(j\gg1)}(\delta)$ for $j = 1$ at $\kappa = 0.001$ (blue dots), $\kappa = 0.01$((red dashed line), and $\kappa = 0.1$ (green dashed-dotted line), see text. The full red line corresponds to ${}^{\mathrm{ANCCD}}N^{(j)}(\delta)/{}^{\mathrm{ACClCD}}N^{(j\gg1)}(\delta)$. Marked are the threshold and reference values of the scaled dipole moment δ.

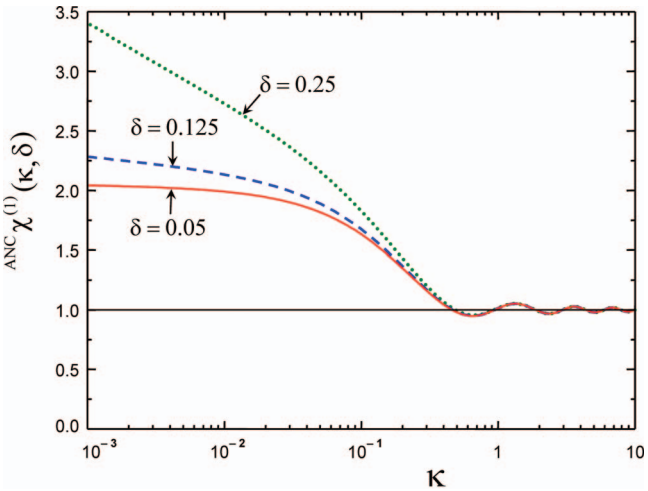

FIG. 7. Scaled rate coefficients ${}^{\mathrm{ANC}}\chi^{(j)}(\kappa, \delta)$, for $j = 1$ and for small values of the scaled dipole moment δ, see Eq. (2.3) ($\delta = 0.05$(full red line), $\delta = 0.125$(dashed blue line), $\delta = 0.25$(dotted green line), κ = scaled wave vector from Eq. (2.3)).

V. BRIDGING THE GAP BETWEEN ULTRA-LOW AND MEDIUM ENERGIES

In the regime of medium (M) collision energies and temperatures, in the absence of the charge–dipole interaction, the rate coefficient is determined by many capture waves. The bridging between the UL and M limits then requires accurate calculations of J, j, n-specific contributions to Eqs. (3.4) and (3.5). In this section we discuss this bridging for a specific choice of the parameter δ for which the UL regime can be described in simple ways. These correspond to small values of δ when ${}^{\mathrm{ANC}}\chi^{(j)}(\kappa, \delta)$ can be calculated within the FW approach, and to large δ from the reference set when ${}^{\mathrm{ANC}}\chi^{(j)}(\kappa, \delta)$ are close to ${}^{\mathrm{ACCI}}\chi^{(j)}(\kappa, \delta)$, i.e., to ACCl rate coefficients extrapolated to small κ beyond the formal validity limit. The general low-energy case will be treated in Paper II[36] of this series.

The ACCl expression for ${}^{\mathrm{ACCI}}\chi^{(j)}(\kappa, \delta)$ is well-known,[19–21] and here we use it in a form appropriate for our discussion as formulated in Ref. 22. Explicitly, the ACCl rate coefficient for capture of rotationally unpolarized symmetric top rotors with rotational quantum number j and effective reduced dipole moment δ reads

$$ {}^{\mathrm{ACCl}}\chi^{(j)}(\kappa, \delta) = \frac{1}{(2j+1)} \sum_{n=-j}^{n=j} \left(1 + \frac{n\delta}{\kappa\sqrt{j(j+1)}}\right) \times \Theta\left(1 + \frac{n\delta}{\kappa\sqrt{j(j+1)}}\right). \quad (5.1) $$

For $j \gg 1$, Eq. (5.1) becomes

$$ {}^{\mathrm{ACCl}}\chi^{(j\gg1)}(\kappa, \delta) = 1 + \left(-\frac{1}{2} + \frac{\kappa}{4\delta} + \frac{\delta}{4\kappa}\right)\Theta(1 - \kappa/\delta), \quad (5.2) $$

where $\Theta(x)$ denotes the step function of x. For $\kappa < \delta$, the consecutive opening of capture channels produces slight undulations of ${}^{\mathrm{ACCl}}\chi^{(j)}(\kappa, \delta)$ in its dependence on κ, where charge–dipole and charge–induced dipole interactions unevenly contribute to the capture. The undulations disappear for large j as given by Eq. (5.2). The significance of undulations can be judged from the ratio of ${}^{\mathrm{ACCl}}\chi^{(j)}(\kappa, \delta)/{}^{\mathrm{ACCl}}\chi^{(j\gg1)}(\kappa, \delta)$, as given by Eqs. (5.1) and (5.2): the maximum deviation from unity occurs for $j = 1$ and amounts to about 6%.

The ANC expression ${}^{\mathrm{ACCI}}\chi^{(j)}(\kappa, \delta)$ for small δ and κ is given by the FW expression from Ref. 22 or from Eq. (4.11). It can be extrapolated to larger κ by generalizing the approximation suggested in Ref. 27 for capture in the case of charge–induced dipole interaction. Explicitly, it reads

$$ {}^{\mathrm{ANC}}\chi^{(j)}_{\mathrm{app}}(\kappa, \delta)\big|_{\delta<1} = \max\{{}^{\mathrm{FW}}\chi_s(\kappa, \delta), {}^{\mathrm{AC}}\chi^{(j)}(\kappa, \delta)\}. \quad (5.3) $$

For $j = 1$, plots of ${}^{\mathrm{ANC}}\chi^{(1)}(\kappa, \delta)$ are shown in Fig. 7.

For $\delta = 0.05$, at small κ one sees the convergence of ${}^{\mathrm{ANC}}\chi^{(1)}(\kappa, \delta)$ to the Vogt-Wannier limit ${}^{\mathrm{VW}}\chi^{(j)} = 2$, indicating a virtually complete quenching of the charge–dipole interaction by Coriolis coupling. The slight overshoot of the VW limit, seen at $\kappa = 10^{-3}$, indicates, however, that at still lower energies the rate coefficient diverges as required by the threshold behavior for the FW limit, see Eq. (4.12). For higher δ (but still $\delta \ll 1$), the rate coefficients are larger due to the increased coupling of **j** to **R**, and their divergence for $\kappa \to 0$ is clearly seen. For large κ, the rate coefficients oscillate with diminishing amplitude about the Langevin limit $\chi = 1$. This feature is due to the consecutive opening of new capture cannels specified by J. However, at $\kappa = \delta/\sqrt{2}$ one does not see any feature which could be related to the classical opening of a charge–dipole capture channel in ${}^{\mathrm{ACCI}}\chi^{(1)}$.

The comparison between ANC and ACCl rate coefficients for large δ is facilitated by the observation that the ANCUL and ACCl rates extrapolated to UL limit, i.e., ${}^{\mathrm{ACClUL}}\chi^{(j)}(\kappa, \delta) = .{}^{\mathrm{ACCI}}\chi^{(j)}(\kappa, \delta)|_{\kappa\ll\delta} = {}^{\mathrm{ACClCD}}N^{(j)}(\delta)/2\kappa$, become nearly equal to each other for the reference set of δ,

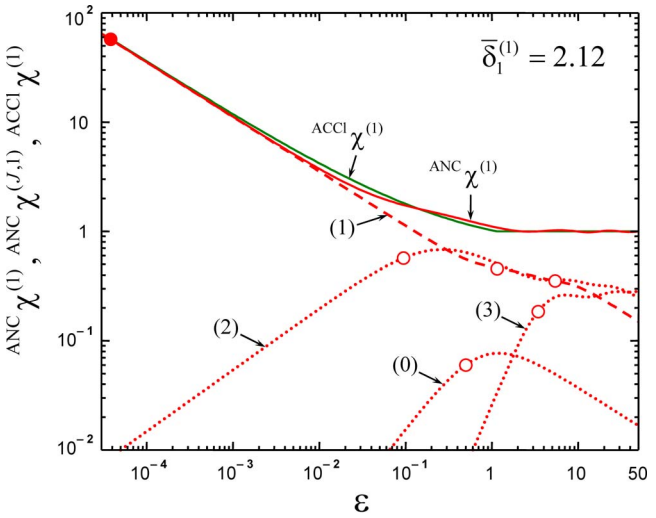

FIG. 8. Total and partial rate coefficients for $j = 1$ and $\delta = {}^{R}\delta_{-1}^{(1,1)} = 2.12$ (the full lines give $^{ANC}\chi^{(1)}(\varepsilon, {}^{R}\delta_{-1}^{(1,1)})$(red) and $^{ACCl}\chi^{(1)}(\varepsilon, {}^{R}\delta_{-1}^{(1,1)})$ (green), the dashed line corresponds to the partial contribution from the lowest capture channel $J = 1$, and the dotted lines to partial contributions from higher capture channels; the curves are labeled by J values; the open circles indicate the classical opening of the first partial channel from a (J, j, n) triad, the filled circle marks the ANC contribution from the $(1, 1, -1)$ triad in the limit $\varepsilon \to 0$; it coincides with the ACCl rate coefficient).

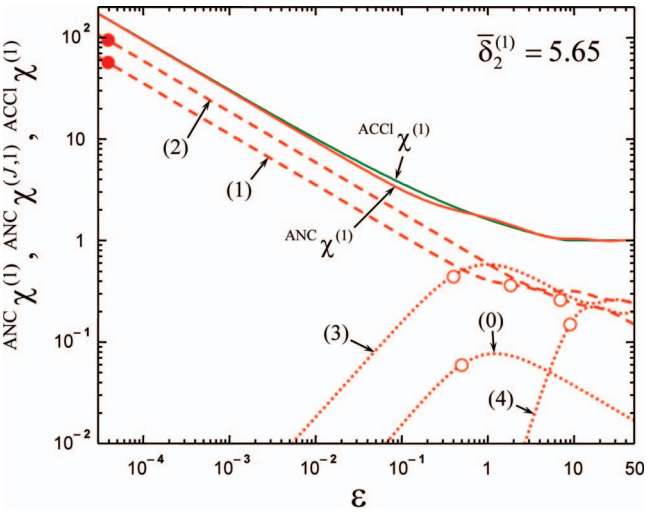

FIG. 9. As Fig. 8, but for $\delta = {}^{R}\delta_{-1}^{(2,1)} = 5.65$ (the full lines give $^{ANC}\chi^{(1)}(\varepsilon, {}^{R}\delta_{-1}^{(2,1)})$ and $^{ACCl}\chi^{(1)}(\varepsilon, {}^{R}\delta_{-1}^{(2,1)})$, the dashed lines correspond to the partial contribution for the two lowest capture channels $J = 1$ and $J = 2$; the filled circles mark the ANC contributions from the $(1, 1, -1)$ and $(2, 1, -1)$ triads in the limit $\varepsilon \to 0$; their sum coincides with the ACCl rate coefficient).

see Fig. 6. Then one can write

$$^{ANC}\chi^{(j)}\left(\kappa, {}^{R}\delta_n^{(J,j)}\right)\Big|_{\kappa\ll 1} \approx {}^{ACCl}\chi^{(j)}\left(\kappa, {}^{R}\delta_n^{(J,j)}\right)\Big|_{\kappa\ll 1}. \quad (5.4)$$

On the other hand, for $\kappa \gg 1$, one has

$$^{ANC}\chi^{(j)}\left(\kappa, {}^{R}\delta_n^{(J,j)}\right)\Big|_{\kappa\gg 1} = {}^{ACCl}\chi^{(j)}\left(\kappa, {}^{R}\delta_n^{(J,j)}\right)\Big|_{\kappa\gg 1} = 1. \quad (5.5)$$

The comparison of the two limiting expressions of Eqs. (5.4) and (5.5) suggests that $^{ANC}\chi^{(j)}(\kappa, {}^{R}\delta_n^{(J,j)})$ may be rather close to $^{ACCl}\chi^{(j)}(\kappa, {}^{R}\delta_n^{(J,j)})$ for all values of κ. Then the difference between $^{ANC}\chi^{(j)}(\kappa, {}^{R}\delta_n^{(J,j)})$ and $^{ACCl}\chi^{(j)}(\kappa, {}^{R}\delta_n^{(J,j)})$ is expected to be due only to the quantum nature of the contributions from the higher partial waves, and not from the sigmoid effect (see Eq. (4.13)). This is illustrated in Figs. 8 for the case $j = 1$ and $\delta = {}^{R}\delta_{-1}^{(1,1)} = 2.12$ when one channel is completely open in the UL range.

Shown are the plots of $^{ANC}\chi^{(1)}(\varepsilon, {}^{R}\delta_{-1}^{(1,1)})$ and $^{ACCl}\chi^{(1)}(\varepsilon, {}^{R}\delta_{-1}^{(1,1)})$, as well as the partial rate coefficients $^{ANC}\chi_n^{(J,1)}$ which include contributions from different n channels. The global maxima of the plots $^{ANC}\chi^{(J,1)}(\varepsilon, \bar{\delta}_1^{(1)})$ roughly correspond to the classical opening of the first channel from the triad $(J, 1, n)$, while the local maxima and the inflection points at higher energies signal the opening of other n-channels. The energies of these points are close to the energies of the classical opening of the respective channels $\varepsilon_n^{(J,1)}(\bar{\delta}_1^{(1)}) = ({}^{ANC}c_n^{(J,1)}(\bar{\delta}_1^{(1)}))^2/8$ which are indicated by open circles. The filled circle in the UL range corresponds to the single open channel $(1, 1, -1)$. Fig. 9 presents similar plots for $\delta = {}^{R}\delta_{-1}^{(2,1)} = 5.65$ when two capture channels are open in the UL energy range (two filled circles).

We finally note that, for values of δ noticeably different from ${}^{R}\delta_n^{(J,j)}$ (especially for δ close to the threshold values ${}^{ANC}\delta_n^{(J,j)}$), the difference between $^{ANC}\chi^{(j)}(\varepsilon, \delta)$ and $^{AC}\chi^{(j)}(\varepsilon, \delta)$ may become larger. Examples of such cases are discussed in Paper II[36] of this series which also presents thermally averaged rate coefficients for a range of δ as well as the application of the ANC approach to the capture of CH_3D by ions.

VI. CONCLUSIONS

The complex formation in ion-molecule collisions often represents a separate stage of the elastic, inelastic, and reactive events. However, even this stage, described usually as a half-collision, is accompanied by a host of inelastic processes occurring on the way to the complex boundary. In this respect, the dynamics of complex formation in collisions of a dipolar isotropically polarizable symmetric rotors with ions represent a rather simple problem that can be solved completely in the quantum case which is of general interest in the context of the physics of cold molecules (see, e.g., Ref. 35). The simplification comes from the applicability of the weak-field approximation for the molecule–ion interaction, from the adiabatic approximation for the rotational transitions in a molecule, and from the separation of the radial and rotational motion of the colliding partners.

Under these conditions, the capturer dynamics is described as uncoupled events occurring in the field of axially nonadiabatic channel (ANC) potentials that include the anisotropic charge–dipole and Coriolis interactions as well as the isotropic charge–induced dipole interaction. The ANC potentials are calculated in the adiabatic approximation with respect to transitions between different rotational states of the top and in the weak-field limit of the charge–dipole interaction. In scaled, reduced, variables δ, ρ defined by Eq. (2.3) the mutually uncoupled scaled potentials $\upsilon(\rho, c)$ of Eq. (3.2) depend on the parameters c. The latter represent a set of eigenvalues of the ANC interaction matrix which depend on

the quantum number of the total angular momentum $J$of the colliding partners, on the adiabatic quantum numbers j of the intrinsic angular momentum of the top, on an additional quantum number n that specifies the ANC channel for a given J, j pair, and finally on the interaction parameter δ. The solution of the wave equation with the appropriate capture boundary conditions determines the capture probabilities and the ANC energy-dependent capture rate coefficient. The latter, ${}^{\rm ANC}\chi$, scaled to their Langevin counterpart $\chi = 1$, depend on the angular momentum of the top j, the scaled dipole moment δ in a given rotational state j, k, and on the scaled collision energy $\varepsilon = E/E_L$ with E_L defined in Eq. (2.3), i.e., ${}^{\rm ANC}\chi \equiv {}^{\rm ANC}\chi^{(j)}(\varepsilon, \delta)$. This paper presented calculations of ${}^{\rm ANC}\chi^{(j)}(\varepsilon, \delta)$ at ultralow collision energies and described the passage to medium energies which made the quantum/classical correspondence quite transparent. In this way, the present treatment fills the gap between the limiting cases elaborated earlier, such as the classical adiabatic channel (AC) treatment (valid for $\kappa \gg 1$ and $\delta \gg 1$),[19–21] the quantum FW treatment (valid for $\kappa \ll 1$ and $\delta < 1$),[22] and the quantum treatment for an isotropic interaction that bridges the gap between the Langevin and Vogt-Wannier limits (valid for arbitrary κ and $\delta = 0$).[32] The ANC capture dynamics elaborated here illustrates the partial coupling of the molecular angular momentum to the collision axis for the charge–dipole interaction (interplay between the R^{-2} channel potentials and the R^{-2} Coriolis coupling) thus supplementing previous studies of a gradual locking for charge–quadrupole and resonance dipole–dipole interactions (interplay between the R^{-3} channel potentials and the R^{-2} Coriolis coupling) and nearly sudden locking for steeper channel potentials proportional to R^{-n} with $n > 3$. Specific examples of capture events of the described nature with noticeable quantum effects are discussed in Paper II[36] of this series with reference to collisions between isotopically substituted methane molecules and different ions.

ACKNOWLEDGMENTS

Financial support of this work by the EOARD Grant Award FA 8655-11-1-3077 is gratefully acknowledged.

[1] M. Quack and J. Troe, Ber. Bunsenges. Phys. Chem. **78**, 240 (1974); **79**, 170 (1975); **79**, 469 (1975).
[2] M. Quack and J. Troe, in *Encyclopedia of Computational Chemistry*, edited by P. V. Schleyer, N. L. Allinger, T. Clark, J. Gasteiger, and P. A. Kollmann (Wiley Chichester, UK, 1998), Vol. 4, p. 2708.
[3] J. Troe, in *State selected and State–to–State Ion–Molecule Reaction Dynamics, Part 2: Theory*, edited by M. Baer and C. Y. Ng (Wiley, New York, 1992); Adv. Chem. Phys. Ser. **82**, 485 (1992).
[4] K. Sakimoto and K. Takayanagi, J. Phys. Soc. Jpn. **48**, 2076 (1980).
[5] D. R. Bates, Proc. R. Soc. London, Ser. A **384**, 289 (1982).
[6] D. C. Clary, Mol. Phys. **54**, 605 (1985).
[7] M. Ramillon and R. McCarroll, J. Chem. Phys. **101**, 8697 (1994).
[8] N. Andersen and K. Bartschat, *Polarization, Alignment, and Orientation in Atomic Collisions* (Springer, New York, 2001).
[9] A. Berengolts, E. I. Dashevskaya, E. E. Nikitin, and J. Troe, Chem. Phys. **195**, 271 (1995); **195**, 283 (1995).
[10] V. Aquilanti, S. Cavalli, and G. Grossi, Z. Phys. D **36**, 215 (1996).
[11] P. S. Shternin and O. S. Vasyutinskii, J. Chem. Phys. **128**, 194314 (2008).
[12] V. V. Kuznetsov, P. S. Shternin, and O. S. Vasyutinskii, J. Chem. Phys. **130**, 134312 (2009).
[13] E. I. Dashevskaya, I. Litvin, E. E. Nikitin, and J. Troe, Mol. Phys. **108**, 873 (2010).
[14] M. Auzinsh, E. I. Dashevskaya, I. Litvin, E. E. Nikitin, and J. Troe, J. Phys. Chem. A **115**, 5027 (2011).
[15] E. E. Nikitin and J. Troe, J. Chem. Phys. **92**, 6594 (1990).
[16] A. I. Maergoiz,. E. E. Nikitin, J. Troe, and V. G. Ushakov, J. Chem. Phys. **117**, 4201 (2002).
[17] E. I. Dashevskaya, I. Litvin, E. E. Nikitin, I. Oref, and J. Troe, J. Phys. Chem. A **108**, 8703 (2004).
[18] E. E. Nikitin and J. Troe, Phys. Chem. Chem. Phys. **7**, 1540 (2005).
[19] J. Troe, J. Chem. Phys. **87**, 2773 (1987).
[20] S. C. Smith and J. Troe, J. Chem. Phys. **97**, 5451 (1992).
[21] J. Troe, J. Chem. Phys. **105**, 6249 (1996).
[22] M. Auzinsh, E. I. Dashevskaya, E. E. Nikitin, and J. Troe, "Quantum capture of charged particles by rapidly rotating symmetric top molecules with small dipole moments. Analytical comparison of the fly-wheel and adiabatic channel limits," Mol. Phys. (in press).
[23] F. A. Gangemi, J. Chem. Phys. **39**, 3490 (1963).
[24] S. C. Wofsy, J. S. Muenter, and W. Klemperer, J. Chem. Phys. **53**, 4005 (1970).
[25] X. R. Böhmer, U. Giebenhain, and A. Loidl, Mol. Phys. **82**, 531 (1994).
[26] Y. H. Hollenstein, R. R. Marquardt, M. Quack, and M. A. Suhm, J. Chem. Phys. **101**, 3588 (1994).
[27] A. I. Maergoiz,. E. E. Nikitin, J. Troe, and V. G. Ushakov, J. Chem. Phys. **105**, 6263 (1996).
[28] T. F. O'Malley, L. Spruch, and L. Rosenberg, J. Math. Phys. **2**, 491 (1961).
[29] R. M. Spector, J. Math. Phys. **5**, 1185 (1964).
[30] N. A. W. Holzwarth, J. Math. Phys. **14**, 191 (1973).
[31] M. J. Moritz, Ch. Eltschka, and H. Friedrich, Phys. Rev. A **63**, 042102 (2001).
[32] E. I. Dashevskaya, A. I. Maergoiz, J. Troe, I. Litvin, and E. E. Nikitin, J. Chem. Phys. **118**, 7313 (2003).
[33] L. D. Landau and E. M. Lifshitz, *Quantum Mechanics* (Pergamon Press, Oxford, 1977).
[34] I. I. Fabrikant and H. Hotop, Phys. Rev. A **63**, 022706 (2001).
[35] *Cold Molecules*, edited by R. V. Krems, W. C. Stwalley, and B. Friedrich (CRS Press, New York, 2009).
[36] M. Auzinsh, E. I. Dashevskaya, I. Litvin, E. E. Nikitin, and J. Troe, "Quantum effects in the capture of charged particles by dipolar polarizable symmetric top molecules. II. Interplay between electrostatic and gyroscopic interactions," J. Chem. Phys. (submitted).